Journal of Virological Methods 224 (2015) 58–66

Contents lists available at ScienceDirect

Journal of Virological Methods

journal homepage: www.elsevier.com/locate/jviromet

Optimization of Droplet Digital PCR from RNA and DNA extracts with direct comparison to RT-qPCR: Clinical implications for quantification of Oseltamivir-resistant subpopulations

Sean C. Taylor[a,*], Julie Carbonneau[b], Dawne N. Shelton[c], Guy Boivin[b]

[a] Bio-Rad Laboratories Canada, Inc., 1329 Meyerside Drive, Mississauga, ON, Canada L5T1C9
[b] CHU of Quebec and Laval University, Quebec City, QC, Canada
[c] Digital Biology Center, Bio-Rad Laboratories, Pleasanton, CA, USA

Article history:
Received 22 November 2014
Received in revised form 21 July 2015
Accepted 19 August 2015
Available online 24 August 2015

Keywords:
Droplet Digital PCR
Influenza virus
Experimental optimization
RT-qPCR
ddPCR

A B S T R A C T

The recent introduction of Droplet Digital PCR (ddPCR) has provided researchers with a tool that permits direct quantification of nucleic acids from a wide range of samples with increased precision and sensitivity versus RT-qPCR. The sample interdependence of RT-qPCR stemming from the measurement of C_q and ΔC_q values is eliminated with ddPCR which provides an independent measure of the absolute nucleic acid concentration for each sample without standard curves thereby reducing inter-well and inter-plate variability. Well-characterized RNA purified from H275-wild type (WT) and H275Y-point mutated (MUT) neuraminidase of influenza A (H1N1) pandemic 2009 virus was used to demonstrate a ddPCR optimization workflow to assure robust data for downstream analysis. The ddPCR reaction mix was also tested with RT-qPCR and gave excellent reaction efficiency (between 90% and 100%) with the optimized MUT/WT duplexed assay thus enabling the direct comparison of the two platforms from the same reaction mix and thermal cycling protocol. ddPCR gave a marked improvement in sensitivity (>30-fold) for mutation abundance using a mixture of purified MUT and WT RNA and increased precision (>10 fold, $p < 0.05$ for both inter- and intra-assay variability) versus RT-qPCR from patient samples to accurately identify residual mutant viral population during recovery.

1. Introduction

Droplet Digital PCR (ddPCR) uses emulsion chemistry to partition 20 μL nucleic acid samples into approximately 20,000 oil-encapsulated nanodroplets to produce data that surpasses the precision of RT-qPCR with equivalent or much higher sensitivity (Hindson et al., 2011, 2013). Applications such as rare allele or mutation detection in a complex background or quantification of nucleic acids in samples with high levels of contaminants benefit from ddPCR relative to qPCR (Sanmamed et al., 2015; Rački et al., 2014). Another major advantage of ddPCR is the elimination of interwell, intersample and interplate dependence on data acquisition permitting sample testing throughout a study. For RT-qPCR, the interdependence of samples and/or standards (based on C_T and ΔC_T values (now termed C_q for minimum information for publication of quantitative real-time PCR experiments (MIQE) compliance (Bustin et al., 2009)) ideally requires running all samples per target on the same plate to minimize technical error. In fact, obtaining reproducible data for the same sample distributed between multiple labs has been a significant challenge with variability up to three to four logs with RT-qPCR (Zhang et al., 2007; Hayden et al., 2008). Finally, multiplexing reactions is challenging with RT-qPCR because of its dependence on reaction efficiency as opposed to ddPCR for which data is acquired at end point and therefore virtually efficiency independent to permit the plexing of assays with much greater ease (Persson et al., 2005; McDermott et al., 2013).

ddPCR has been recently compared to qPCR for detection of viral nucleic acids with improved precision and elimination of standard curves (Brunetto et al., 2014; Zhao et al., 2013; Leibovitch et al., 2014). For many viral strains, resistance to antiviral drug treatment is conferred through spontaneous point mutations. For immunocompromised patients, the accurate detection of these mutations is critical to effective treatment (Pizzorno et al., 2011; Ghedin et al., 2012; Corcioli et al., 2014). RT-qPCR has demonstrated a limit of detection of about 10% for influenza virus mutation abundance (ratio of point mutant (MUT)/(MUT + wild type (WT)) × 100) (Escuret et al., 2014). Similar results have been shown with circulating DNA obtained from cancer patients and from solid tumour

* Corresponding author. Tel.: +1 800 268 0213; fax: +1 888 913 9779.
E-mail address: sean_taylor@bio-rad.com (S.C. Taylor).

http://dx.doi.org/10.1016/j.jviromet.2015.08.014

samples (Angulo et al., 2010; Thomas et al., 2006). Although this limit of detection is acceptable for categorizing a disease state, it is not adequate for disease monitoring in cancer or for immunocompromised patients with drug-resistant infection (Oxnard et al., 2014; Watzinger et al., 2004). Here, well-characterized, purified RNA samples from influenza A(H1N1)pdm09 virus were used to demonstrate the key steps to optimize ddPCR experiments. The optimized assay was then applied to the detection of the most frequent influenza mutation (H275Y) conferring resistance to Oseltamivir in a mixture of RNA from purified mutant and wild type recombinant viruses and from patient samples over the course of influenza infection.

2. Materials & methods

2.1. RNA samples

2.1.1. Purified RNA samples

RNA was extracted from recombinant influenza A(H1N1)pdm09 virus (GenBank FN434457 to FN434464) rescued by reverse genetics using bidirectional pLLBA plasmids as previously described (Pizzorno et al., 2011). The H275Y NA mutant was generated by performing site-directed mutagenesis on the plasmid containing the NA gene.

2.1.2. Patient RNA samples

To compare the percent mutation abundance between ddPCR and RT-qPCR platforms, nucleic acid extracts of patient samples were collected over time. Influenza A(H1N1)pdm09 virus infection was diagnosed on January 5, 2011 in a 31 month-old boy with medulloblastoma who received consolidation chemotherapy in preparation of an autologous bone marrow transplantation (Ghedin et al., 2012). The child was treated with Oseltamivir (30 mg BID) from January 6 to 28 and then with Zanamivir (25 mg inhaled 4 times daily) until negative RT-qPCR results were obtained on February 17, 2011. The patient recovered from his infection without complication. RNA was extracted from sequential nasopharyngeal aspirates (NPA) using the MagNA Pure total nucleic acid isolation kit (Roche Applies Science) as reported (Ghedin et al., 2012). The RNA from the patient sample set to assess intra-assay variability (i.e., same RNA sample pipetted into triplicate wells of the same plate (Table 1)) was extracted on a different day by a different operator than the RNA (from the same patient samples) used to assess inter-assay variability (i.e., same RNA samples frozen and thawed at different times and tested in three different plates (Table 2)).

2.2. Primers and probes

The primers and probes targeted the H275 (WT) and H275Y (MUT) variants of influenza A(H1N1)pdm09 virus as previously described (Ghedin et al., 2012) and were purchased from Integrated DNA Technologies (Coralville, Iowa).

2.3. RT-qPCR

For patient samples tested for intra-assay variability (see Section 2.1.2), the one-step RT-PCR mixture was prepared in a 25 μL reaction volume containing 6.25 μL of TaqMan Fast Virus 1-Step Master Mix (Applied Biosystems, Foster City, CA), 0.8 μL of both the reverse and the forward primers, 1.0 μL of each probe and 4.0 μL of RNA extract (Pinilla et al., 2012). The amplification process was performed in a LightCycler 480 real-time thermocycler (Roche Applied Science, Mannheim, Germany) under the following cycling conditions: 60 °C for 30 min (RT) and 95 °C for 5 min (DNA polymerase activation), followed by 45 cycles of 95 °C for 20 s (denaturation) and 62 °C for 1 min (annealing). For all reactions split between RT-qPCR and ddPCR, the amplification process was performed in a LightCycler 480 real-time thermocycler using the optimized ddPCR cycling protocol and supermix (see Section 2.7).

2.3.1. Assessment of ddPCR reaction mix for RT-qPCR

Purified viral RNA (see Section 2.1.1.) from the WT and MUT recombinant strains were tested in RT-qPCR using the ddPCR reaction mix to assess primer reaction efficiency and linear dynamic range of RNA samples. Serial, 2-fold dilutions of samples ($\approx 10^5$ diluted to 10^3 copies per reaction) in 10 mM, nuclease-free Tris buffer (pH 7.5) were used as template with the duplexed WT/MUT primer/probes using the ddPCR reaction supermix and associated cycling protocol (see Section 2.4) for detection of WT/MUT virus in both RT-qPCR and ddPCR (Supplemental Fig. S1).

2.4. ddPCR

Twenty microliters of each reaction mix was converted to droplets with the QX200 droplet generator (Bio-Rad). Droplet-partitioned samples were then transferred to a 96-well plate, sealed and cycled in a C1000 deep well Thermocycler (Bio-Rad) under the following cycling protocol: 60 °C for 30 min (RT) and 95 °C for 5 min (DNA polymerase activation), followed by 40 cycles of 95 °C for 30 s (denaturation) and 55 °C for 1 min (annealing) followed by post-cycling steps of 98 °C for 10 min (enzyme inactivation) and an infinite 10 degree hold. The cycled plate was then transferred and read in the FAM and HEX channels using the QX200 reader (Bio-Rad) either the same or the following day post-cycling.

2.5. Primer/probe thermal gradient optimization

Serial 10-fold dilutions (10^4 to 10^6 copies per reaction) in 10 mM, nuclease-free Tris buffer (pH 7.5) of purified viral RNA from the WT, MUT and mixtures of WT/MUT recombinant strains were used as template to assess the optimal annealing temperature of the individual and duplexed primer/probes. The standard ddPCR cycling program was modified by replacing the annealing temperature step with a thermal gradient between 52 °C and 64 °C for 1 min extension time (Fig. 1).

2.6. Standard curve and controls for ddPCR

A 1/2 dilution of the MUT RNA in a constant WT background (Fig. 2B) and the inverse experiment with diluted WT in constant MUT background (data not shown) was produced. Duplicate control samples containing either MUT or WT RNA were also tested with the duplexed MUT/WT primer/probes to determine the level of crosstalk and the lower limit of reliable quantification for the duplex assay (Fig. 2A2). A traditional no template control was also sampled (Fig. 2A3).

2.7. Split reactions between RT-qPCR and ddPCR

For purified RNA samples and patient samples tested for intra-assay variability, a total of 50 μL reaction mix was prepared using 25 μL of ddPCR supermix (One-Step RT-ddPCR Kit for Probes for RNA (Bio-Rad)), primers and probes to a final concentration of 800 nM and 200 nM, respectively, and influenza virus RNA at a concentration of 0.33 pg or 1×10^5 copies per well. Twenty μL aliquots of these reaction mixes were used to quantify samples by RT-qPCR and ddPCR under optimized ddPCR cycling conditions (see Section 2.4). For patient samples tested for inter-assay variability, a 44 μL reaction mix was prepared from 22 μL of ddPCR supermix, primers and probes and RNA as above. Twenty μL aliquots of these reaction

Table 1
Assessing intra-assay variability between ddPCR and RT-qPCR. Triplicate experiments for both ddPCR and RT-qPCR were performed as typical technical replicates from the same RNA samples extracted from a set of patient samples and pipetted on the same plate for each respective platform. Identical RNA samples were tested with RT-qPCR and ddPCR using different PCR reagents and cycling conditions (see Sections 2.3 and 2.4). H: wild type; Y: H275Y point mutant; %: mean mutation abundance for H (copies of H/(copies of H + Y) × 100) for triplicate replicates; %CV: coefficient of variation between replicates ((standard deviation/mean) × 100); *p*-value: statistical significance of the mean % mutation abundance between successive sampling dates. Arrows indicate the successive pairs of sampling dates compared for statistical analysis.

	RT-qPCR						ddPCR						
Nasopharyngeal swab date	H			Y			H			Y			Antiviral therapy
	%	% CV	p-value	%	% CV	p-value	%	% CV	p-value	%	% CV	p-value	
1/5/2011	99.9	56.6		0.1	45.0		98.2	5.0		1.8	8.9		none
1/10/2011	99.7	74.2	0.997	0.3	89.2	0.242	98.0	0.9	0.9382	2.0	10.0	0.2879	Oseltamivir
1/17/2011	3.1	109.7	0.087	96.9	70.2	0.070	9.4	8.0	0.0001	90.6	5.2	0.0001	Oseltamivir
1/28/2011	21.1	62.1	0.083	78.9	48.5	0.710	4.8	11.4	0.0011	95.2	8.0	0.4230	Oseltamivir
2/8/2011	11.5	75.4	0.350	88.5	67.5	0.826	3.8	5.8	0.0324	96.2	4.3	0.8508	Zanamivir
2/17/2011	0.0	0.0		0	0	0	0	0		0	0		Zanamivir

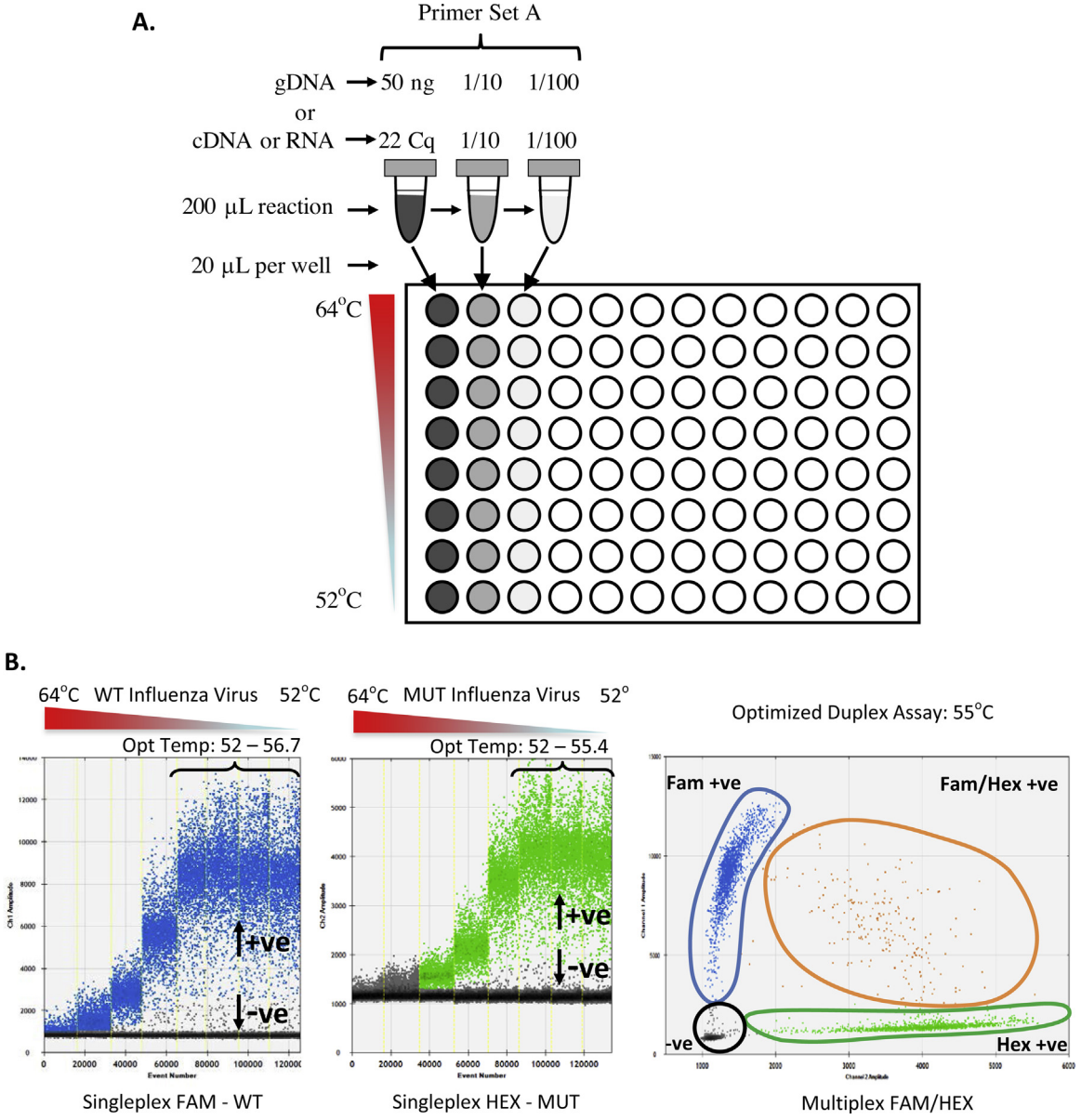

Fig. 1. Combined thermal gradient and sample concentration optimization for primer/probe annealing temperature in single and duplex assays. Schematic for the ddPCR thermal gradient optimization experiment depicting recommended dilutions of cDNA or gDNA and primer annealing temperature range (A). The optimal annealing temperature range and orthogonal 2D amplitude plot are shown for the dilution corresponding to 25 C_q (10^5 copies) from the RT-qPCR data for the MUT, WT and mixed MUT/WT RNA samples which was approximately in the middle of the linear dynamic range for ddPCR (about 250 copies per µL) (B). Droplets color code: Gray: negative; Green: Hex probe for MUT target; Blue: Fam probe for WT target; Orange: double positive droplets containing both MUT and WT targets.

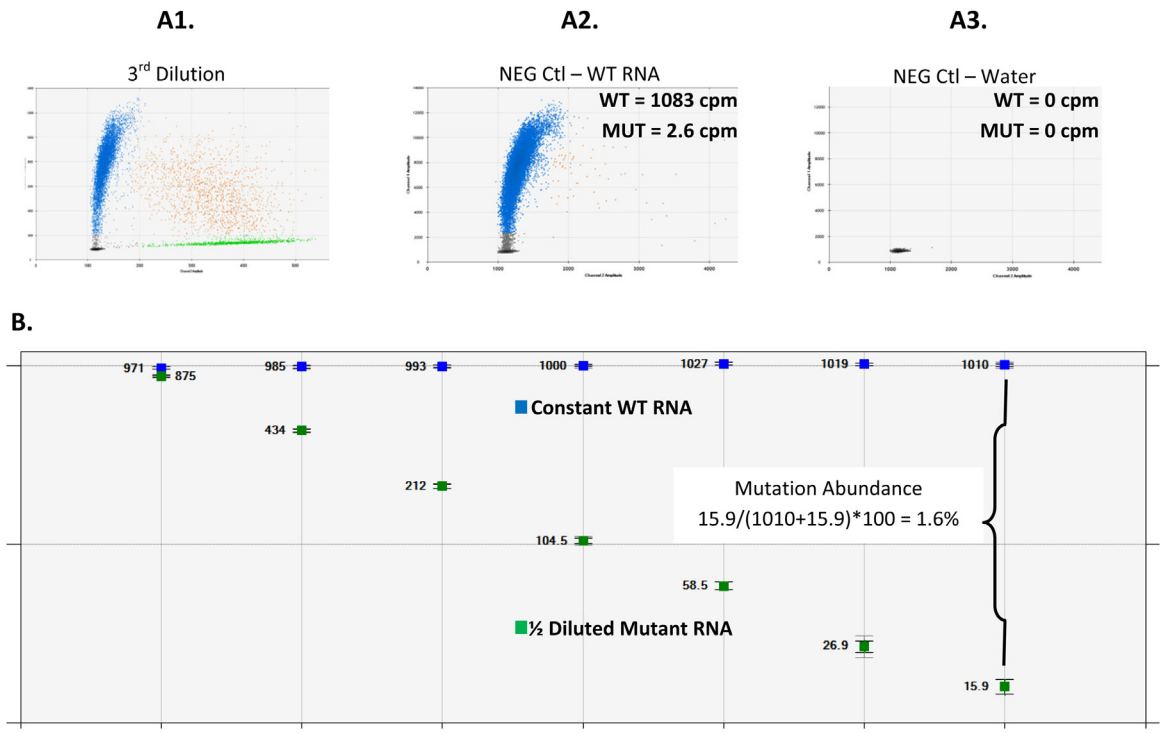

Fig. 2. Validation of the quantitative linear dynamic range for ddPCR. 2D Amplitude plots of the raw data are shown for ddPCR for the third dilution of the MUT/WT dilution series (A1), the negative control sample with WT virus only (A2) and the no template control (water) (A3). A 1/2 dilution series of MUT in a constant WT RNA mixtures were quantified from the ddPCR workflow using the optimized duplex MUT/WT primer probes (B). Each point displays the copies per μL (CPM) for MUT and WT in each sample. Error bars indicate the Poisson 95% confidence intervals for each copy number determination. Mutation abundance is calculated by dividing the MUT CPM by the sum of WT and MUT CPM values.

mixes were used to quantify samples by RT-qPCR and ddPCR under optimized ddPCR cycling conditions.

2.8. Percent mutation abundance, statistical analysis and calculation of the coefficient of variation

For both RT-qPCR and ddPCR, the percent mutation abundance was calculated from the mean copy per μL (CPM) of the triplicate replicate patient samples (WT/(MUT + WT) × 100) or (MUT/(MUT + WT) × 100) and summarized with the coefficient of variation (standard deviation/mean × 100). All populations were normally distributed using the Shapiro–Wilk test. A Student *t* individual paired comparisons test was chosen to determine the statistical significance between mean percent mutation abundance of each successive date for patient sampling (De Winter, 2013). A Kendall tau correlation test was applied to the RT-qPCR and ddPCR data to measure the association between mutation abundance data generated for the patient samples tested within each platform and between the different RNA extracts used for intra- and inter-assay variability analysis (Fig. 4).

3. Results

3.1. Using RT-qPCR to assess primer efficiency in the ddPCR reaction mix and to approximate the dilution factor for ddPCR analysis of RNA and cDNA

ddPCR as applied to the QX200 has a quantitative linear dynamic range between 1 and 5000 copies per microliter (ie: 20 to 100,000 copies) and a lower limit of sensitivity of about 4 copies in a single

Table 2
Assessing inter-assay variability between ddPCR and RT-qPCR for independent experiments. Triplicate experiments for both ddPCR and RT-qPCR were performed as independent replicates from fresh extracts of RNA (and different from those tested in Table 1 from the original patient samples). The RNA was frozen and thawed at three different times and assayed on three different plates for both platforms. In order to more directly compare the results between ddPCR and RTqPCR, a single reaction mix was produced for each RNA sample and split between ddPCR and RT-qPCR for each experiment (see Section 2.7). H: wild type; Y: H275Y point mutant; %: mean mutation abundance for H (copies of H/(copies of H + Y) × 100) for triplicate replicates; %CV: coefficient of variation between replicates ((standard deviation/mean) × 100); *p*-value: statistical significance of the mean % mutation abundance between successive sampling dates. Arrows indicate the successive pairs of sampling dates compared for statistical analysis.

	RT-qPCR						ddPCR						
Nasopharyngeal swab date	H			Y			H			Y			Antiviral therapy
	%	% CV	p-value	%	% CV	p-value	%	% CV	p-value	%	% CV	p-value	
1/5/2011	93.2	20.2		6.8	72.1		99.8	26.8		0.2	55.0		none
1/10/2011	89.6	30.7	0.861	10.4	52.9	0.445	98.3	8.6	0.9306	1.7	11.2	0.0003	Oseltamivir
1/17/2011	26.8	34.7	0.020	73.2	36.6	0.017	10.2	4.9	0.0001	89.8	2.9	0.0001	Oseltamivir
1/28/2011	21.8	34.4	0.509	78.2	33.6	0.829	6.7	4.2	0.0005	93.3	6.1	0.3888	Oseltamivir
2/8/2011	22.2	42.8	0.957	77.8	59.4	0.990	4.2	4.3	0.0003	95.8	6.2	0.6255	Zanamivir
2/17/2011	0.0	0.0		0	0	0	0	0		0	0		Zanamivir

20 μL reaction. This corresponds to a range of about 22 to 35 C_q with RT-qPCR but should be tested for specific experiments using a pooled sample from all the experimental conditions. Assessing a serially diluted sample (pooled RNA, cDNA, gDNA) or possibly DNA from a cloned plasmid or PCR product (as a positive control) for each primer/probe set using standard RT-qPCR will reveal the reaction efficiency, linear dynamic range and the approximate dilution factor required to avoid saturation of the ddPCR reaction.

In order to directly compare the RT-qPCR and ddPCR platforms, the ideal experiments would be designed using the same reaction mix and cycling protocol such that the platform (RT-qPCR or ddPCR) represents the only difference between the results. Given that standard RT-qPCR supermixes are not compatible with ddPCR because they leach out of the oil-encased droplets, the ddPCR supermix was assessed for compatibility with RT-qPCR. Both the MUT and WT primer/probes gave optimal reaction efficiencies between 90 and 110% (as defined by the MIQE guidelines) in RT-qPCR using the ddPCR supermix and cycling conditions (Supplemental Fig. S1) supporting its applicability as a unified reagent to compare both platforms. The dilution corresponding to 24 C_q (i.e., 10^6 copies for this experiment) was used as the starting sample with two additional 1/10 dilutions (i.e., 10^5 and 10^4 copies) for primer/probe annealing temperature optimization with ddPCR.

3.2. Primer/probe annealing temperature, RNA concentration and orthogonality of droplet separation in the duplex assay

In a typical optimization experiment, a pooled RNA or cDNA sample (diluted at least 1/10) from all the study sample sets should initially be tested in RT-qPCR with all primers pairs and then diluted to approximately 22 C_q for each target for the ddPCR thermal gradient optimization experiment (Fig. 1A). However, if the C_q value from the 1/10 pooled sample is beyond 22 C_q, then the undiluted, pooled sample should be used as the starting sample for ddPCR optimization. For genomic DNA, 10 to 50 ng of pooled DNA from the study sets should be used for ddPCR optimization (Fig. 1A).

WT and MUT RNA from influenza A(H1N1)pdm09 virus were serially diluted 1/10 and tested with the duplex WT/MUT primer probe set in RT-qPCR for thermal gradient optimization. The sample dilution corresponding to 25 C_q (10^5 copies) was approximately in the middle of the linear dynamic range for ddPCR (about 250 copies per μL) and the optimal range of annealing temperatures giving the largest difference in fluorescence between negative and positive droplets was between 52 °C and 55.4 °C for both MUT and WT primers (Fig. 1B). An optimized annealing temperature of 55 °C was chosen for the subsequent experiments and the duplexed assay gave good, orthogonal separation between the MUT, WT, negative and MUT/WT double positive droplet species in the 2D amplitude plot (Fig. 1B).

3.3. Determination of the linear, quantitative dynamic range for ddPCR and lower limit of quantification

A standard curve with the appropriate negative controls remains the most reliable method to assure that samples are diluted to an appropriate concentration to achieve the highest quality data for most analytical methods including RT-qPCR and even quantitative western blotting (Taylor and Mrkusich, 2014; Taylor et al., 2013). The same holds true for ddPCR where a 1/2 dilution of the MUT RNA in a constant WT background (Fig. 2B) and the inverse experiment with diluted WT in constant MUT background (data not shown) gave the predicted two fold reduction in RNA concentration over the entire range tested. Also, the 2D-amplitude plot from each dilution gave the expected orthogonality for each droplet species (Fig. 2A1). Negative controls were used to assure samples were diluted appropriately (Figs. 2A2 and A3).

3.4. Divergent data between ddPCR and qPCR for quantification of purified RNA samples

qPCR and ddPCR gave highly divergent data with respect to precision and sensitivity. For the 1/2 diluted MUT RNA samples, there was a single C_q difference between the first two samples for RT-qPCR and the remaining dilutions converged at the same C_q value whereas for ddPCR the data closely correlated to the expected 2-fold dilution factor over all seven dilutions. This corresponds to a mutation abundance limit of detection (LOD) of about 50% for RT-qPCR and 1.41% for ddPCR and thus an increase in sensitivity of about 30 fold for this particular duplex influenza assay (Fig. 3).

3.5. Application of ddPCR to quantify viral populations from patient samples with influenza A(H1N1)pdm09 H275Y mutant infection

The relative percent abundance of viral load present in sequential NPA samples of an immunocompromised child for both the WT and MUT virus subpopulations was quantified using RT-qPCR and ddPCR to assess reproducibility and precision (Tables 1 and 2). When one set of RNA samples was tested for intra-assay variability under optimized conditions using the respective RT-qPCR and ddPCR reagents and cycling conditions, the %CV was greater than 10 fold higher (from 45 to 109.7%) for RT-qPCR compared to ddPCR (0.9 to 11.4%) and gave insignificant results between all the samples (p-value > 0.05) for RT-qPCR (Table 1). Similarly, when a second set of RNA extracts from the same patient samples were tested for inter-assay variability using the ddPCR reaction mix and cycling protocol, the %CV of the viral load remained about 10 fold higher with mostly insignificant results for RT-qPCR (Table 2). Alternatively, ddPCR gave precise and significant results (p-value < 0.05) with low variability (Tables 1 and 2).

A Kendall tau correlation test was applied to the RT-qPCR and ddPCR data to measure the association between the different RNA extracts used for intra- and inter-assay variability analysis. There was no significant correlation (p-value = 0.0909; tau = 0.600) between the data sets for RT-qPCR (Fig. 4A) and a strong correlation (p-value = 0.0048; tau = 1.000) between the ddPCR data (Fig. 4B).

4. Discussion

ddPCR permits a multidimensional approach to assay optimization through the examination of both droplet amplitude and scatter coupled with absolute quantification of DNA and RNA concentration. Unlike RT-qPCR where the data are measured from a single amplification curve and a C_q value that is highly dependent on reaction efficiency, primer dimers and sample contaminants, ddPCR is measured at reaction end point which virtually eliminates these potential pitfalls. Despite these benefits, experimental optimization remains a requirement for ddPCR to ensure the final results produce solid, interpretable data (Fig. 1A). The hallmarks of an optimized, duplex assay for ddPCR include: an orthogonal 2D amplitude plot for the duplexed assay (Fig. 1B); a similar measured concentration (within 10%) of target amplicons between the single and duplexed primer/probe assays and between technical replicates taking into account any concentration differences between the samples for each test; optimized assay separation between positive and negative droplets, or maximal fluorescence amplitude indicative of an efficient PCR reaction and typically verified by thermal gradient (Fig. 1B); a standard curve from a serially diluted sample with either single or duplexed primer/probes and appropriate

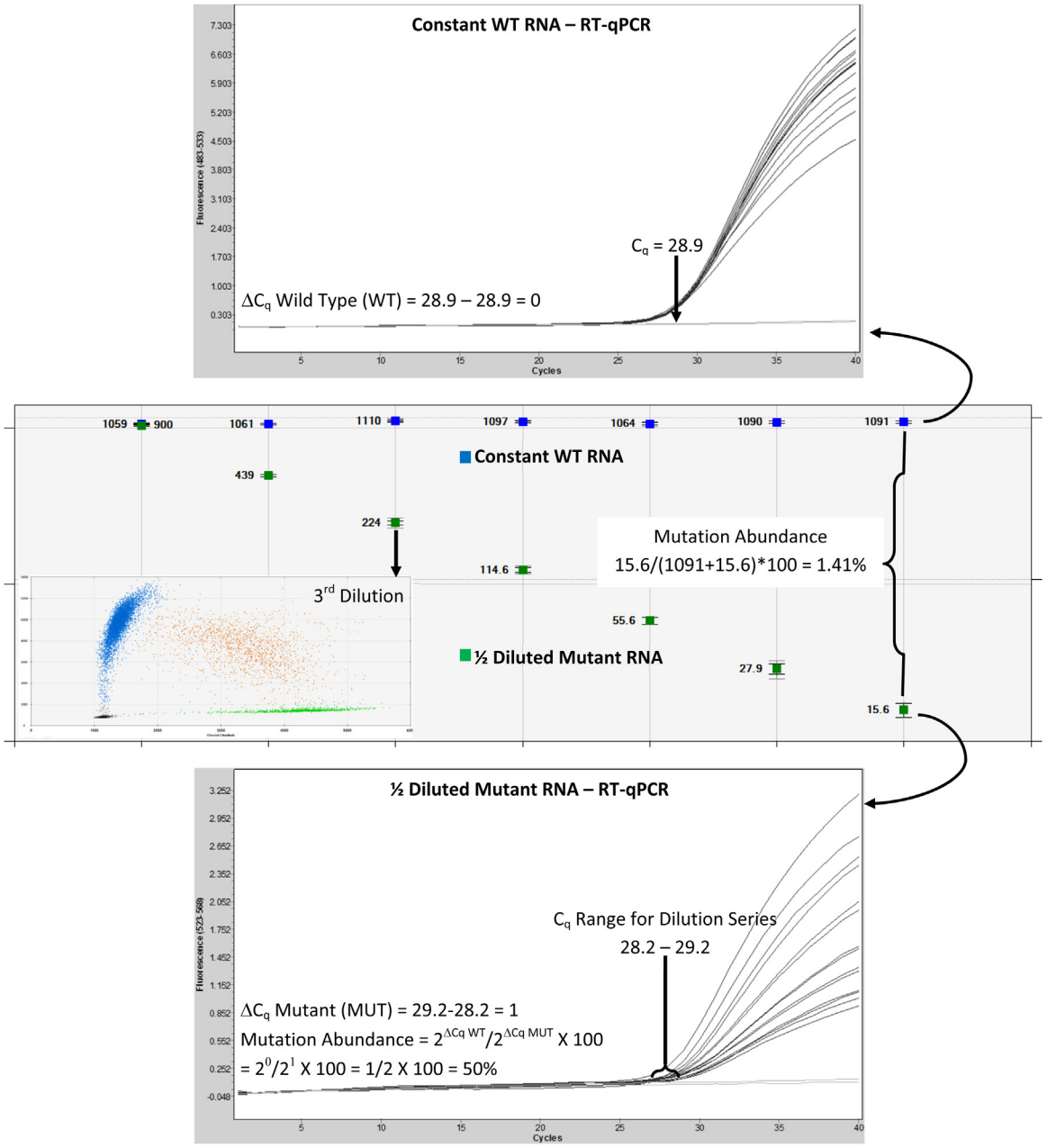

Fig. 3. RT-qPCR and ddPCR from a mock mutation abundance experiment with RNA. A 1/2 dilution series of MUT in a constant WT RNA mixture was quantified from the same mixture of One-Step RT-ddPCR Kit for Probes, duplex MUT/WT primer probes and RNA that was split between ddPCR and RT-qPCR reactions to directly compare the two platforms for data analysis (see Section 2.7). Error bars indicate the Poisson 95% confidence intervals for each copy number determination. 2D Amplitude plots of the raw data are shown for ddPCR for the third dilution of each MUT/WT dilution series (inset). Each point displays the copies per μL (CPM) for MUT and WT in each sample. Mutation abundance is calculated by dividing the MUT CPM by the sum of WT and MUT CPM values.

negative controls to assess the dynamic range and precision of each ddPCR assay (Fig. 2).

Sample partitioning not only improves precision of ddPCR versus RT-qPCR but, in the case of mutation abundance assays, sensitivity is also increased significantly as shown here for the mock mutation abundance experiment where qPCR could not resolve dilutions of MUT RNA in the WT background (Fig. 3). When applied to immunocompromised, influenza patients infected with both the MUT (Y) and WT (H) viral strains, the detection and accurate quantification of the relative abundance of each strain in a duplexed MUT/WT primer/probe assay is critical for appropriate selection of drug treatment regimen. Here, the RT-qPCR results did give a decrease in the WT strain with a concomitant increase in the MUT strain after Oseltamivir treatment between 1/10/2011 and 1/17/2011. However, the high intra-assay variability (%CV), large and unpredictable shifts in mutation abundance post-treatment and statistically insignificant differences between all of the sampling dates (p-value > 0.05) made it challenging to interpret the RT-qPCR data (Table 1). Although the inter-assay variability between the RT-qPCR data was generally lower and gave a statistically significant shift in mutation abundance after Oseltamivir treatment between 1/10/2011 and 1/17/2011 (Table 2), the rest of the sampling dates were not statistically significant. For both sets of experiments, the ddPCR results exhibited a precise shift in population of viral strains versus RT-qPCR with a large shift between the viral populations after Oseltamivir treatment followed by a continued decrease in WT virus with a concomitant increase in the MUT form (Tables 1 and 2). The increased precision and statistical

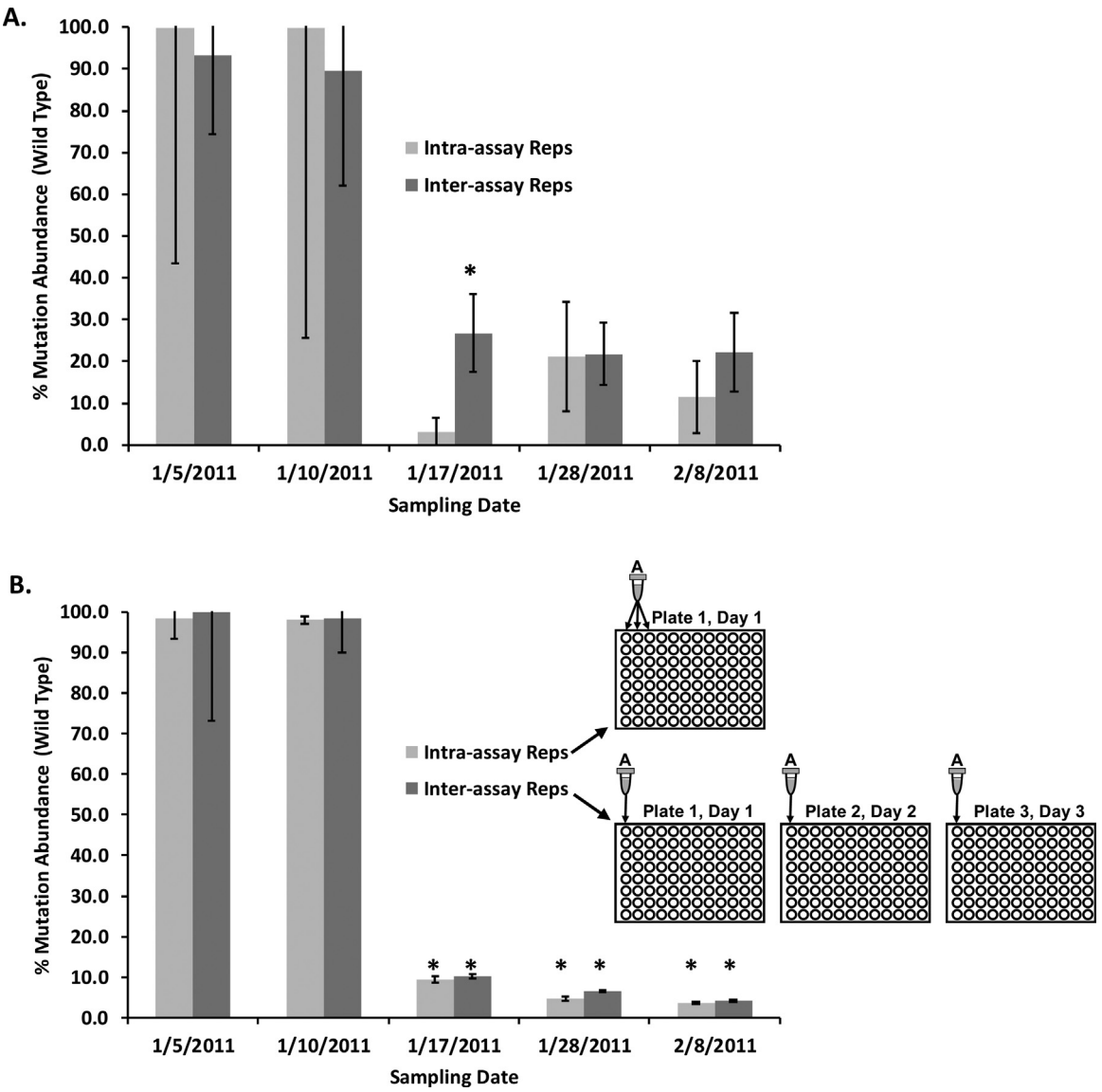

Fig. 4. Assay correlation of RT-qPCR and ddPCR from different RNA extracts (produced from different operators on different dates) of the same patient samples. The mutation abundance of the WT virus population was compared between two independent assays from the same set of influenza infected patient samples for RT-qPCR (A) and ddPCR (B) with data extracted from Tables 1 and 2 for intra-assay and inter-assay replicates respectively. *Intra-assay Reps:* experiment using RNA extracts from three technical replicates pipetted simultaneously from the same, thawed RNA sample at each time point assayed on the same plate at the same time for all samples. *Inter-assay Reps:* experiment from different RNA extracts (different operator extracted the RNA on a different date) of the same patient samples frozen and thawed at three different times and pipetted on three, separate plates for each replicate. For Inter-assay Reps, the reagents and thermal cycling protocols for RT-qPCR and ddPCR were shared between each platform (see Section 2.7) and for Intra-assay Reps, they were specific to each platform (see Sections 2.3 and 2.4). * p-Value < 0.05 between each successive patient sampling time point (see Tables 1 and 2). There was no significant correlation (p-value = 0.0909; tau = 0.600) between the inter- and intra-assay data sets for RT-qPCR (A) and a strong correlation (p-value = 0.0048; tau = 1.000) between the ddPCR data (B).

significance between the successive sampling dates from ddPCR enabled the assessment of treatment with confidence.

ddPCR is an excellent tool for studies requiring sample processing over longer time frames such as weeks, months or years. Also, projects that evolve to include new treatment groups or time points which would be challenging for RT-qPCR where interplate variability can be a significant source of error. Examples of such studies include the collection of rare tumour, tissue or blood samples that may take several months or years to build the study cohort. Other examples could be dynamic patient studies similar to those used here where the results for a given sampling date are required to make decisions for treatment on subsequent dates. Even a simple gene expression experiment that requires comparison of previously collected data with results generated from new experimental conditions would benefit greatly from ddPCR because of the elimination of sample interdependence that contributes to the variability in RT-qPCR. This is exemplified with the influenza patient samples used in this study, where the data acquired from two, independently processed RNA extracts from the same series of patient samples were highly correlated for ddPCR and uncorrelated for RT-qPCR (Fig. 4). Many studies have shown divergent results between laboratories when processing the same samples with RT-qPCR (Zhang et al., 2007; Hayden et al., 2008). The variability in RT-qPCR data is often attributed to the methods used to determine the concentration of standards and the lack of rigor in the production of standard curves for primer validation and absolute quantification (Svec et al., 2015). Consequently, labs are now suggesting the use of ddPCR to validate the concentration of the standards used for RT-qPCR (Hayden et al., 2015).

Although there are now hundreds of publications that underline the benefits of ddPCR, there have been reports concluding that RT-qPCR surpasses ddPCR in sensitivity and precision for clinical samples (Hayden et al., 2013). Although the Hayden study used controlled samples, the reaction conditions between ddPCR and RT-qPCR were much different in terms of cycling protocols, reaction mixes and total volumes which may account for this discrepancy as noted by the authors. This brings to question the level at which these assays were optimized which is unfortunately not possible to assess as is the case for much of the data published with RT-qPCR (Bustin et al., 2013; Dijkstra et al., 2013). Optimizing ddPCR assays will assure excellent data quality, precision and reproducibility for this highly sensitive technique as shown for the detection of drug-resistant influenza populations in the present study.

5. Conclusions

A rigorous approach to ddPCR assay optimization was applied to the quantification of standardized H275 (WT) and H275Y (MUT) strains of influenza A(H1N1)pdm09 virus to directly compare RT-qPCR and ddPCR where the latter gave a 30-fold increase in sensitivity (Fig. 3). The optimized assay was then applied to virus RNA purified from human nasal swab samples where ddPCR gave precise, interpretable and statistically significant results relative to RT-qPCR (Tables 1 and 2). Furthermore, the ddPCR data produced a statistically significant correlation between two sets of independently extracted RNA from the same patient samples (Fig. 4). Based on these results, ddPCR offers a viable alternative to RT-qPCR to obtain precise quantification of nucleic acids extracted from a wide range of samples for reliable interpretation without standard curves or sample interdependence.

Appendix A. Supplementary data

Supplementary data associated with this article can be found, in the online version, at http://dx.doi.org/10.1016/j.jviromet.2015.08.014.

References

Angulo, B., García-García, E., Martínez, R., Suárez-Gauthier, A., Conde, E., Hidalgo, M., López-Ríos, F., 2010. A commercial real-time PCR kit provides greater sensitivity than direct sequencing to detect KRAS mutations: a morphology-based approach in colorectal carcinoma. J. Mol. Diagn. 3, 292–299.

Brunetto, G.S., Massoud, R., Leibovitch, E.C., Caruso, B., Johnson, K., Ohayon, J., Fenton, K., Cortese, I., Jacobson, S., 2014. Digital droplet PCR (ddPCR) for the precise quantification of human T-lymphotropic virus 1 proviral loads in peripheral blood and cerebrospinal fluid of HAM/TSP patients and identification of viral mutations. J. Neurovirol. 4, 341–351.

Bustin, S.A., Benes, V., Garson, J.A., Hellemans, J., Huggett, J., Kubista, M., Mueller, R., Nolan, T., Pfaffl, M.W., Shipley, G.L., Vandesompele, J., Wittwer, C.T., 2009. The MIQE guidelines: minimum information for publication of quantitative real-time PCR experiments. Clin. Chem. 55, 611–622.

Bustin, S.A., Benes, V., Garson, J., Hellemans, J., Huggett, J., Kubista, M., Mueller, R., Nolan, T., Pfaffl, M.W., Shipley, G., Wittwer, C.T., Schjerling, P., Day, P.J., Abreu, M., Aguado, B., Beaulieu, J.F., Beckers, A., Bogaert, S., Browne, J.A., Carrasco-Ramiro, F., Ceelen, L., Ciborowski, K., Cornillie, P., Coulon, S., Cuypers, A., De Brouwer, S., De Ceuninck, L., De Craene, J., De Naeyer, H., De Spiegelaere, W., Deckers, K., Dheedene, A., Durinck, K., Ferreira-Teixeira, M., Fieuw, A., Gallup, J.M., Gonzalo-Flores, S., Goossens, K., Heindryckx, F., Herring, E., Hoenicka, H., Icardi, L., Jaggi, R., Javad, F., Karampelias, M., Kibenge, F., Kibenge, M., Kumps, C., Lambertz, I., Lammens, T., Markey, A., Messiaen, P., Mets, E., Morais, S., Mudarra-Rubio, A., Nakiwala, J., Nelis, H., Olsvik, P.A., Pérez-Novo, C., Plusquin, M., Remans, T., Rihani, A., Rodrigues-Santos, P., Rondou, P., Sanders, R., Schmidt-Bleek, K., Skovgaard, K., Smeets, K., Tabera, L., Toegel, S., Van Acker, T., Van den Broeck, W., Van der Meulen, J., Van Gele, M., Van Peer, G., Van Poucke, M., Van Roy, N., Vergult, S., Wauman, J., Tshuikina-Wiklander, M., Willems, E., Zaccara, S., Zeka, F., Vandesompele, J., 2013. The need for transparency and good practices in the qPCR literature. Nat. Methods 10, 1063–1067.

Corcioli, F., Arvia, R., Pierucci, F., Clausi, V., Bonizzoli, M., Peris, A., Azzi, A., 2014. HA222 polymorphism in Influenza A(H1N1)2009 isolates from Intensive Care Units and ambulatory patients during three influenza seasons. Virus Res. 180, 39–42.

De Winter, J.C.F., 2013. Using the Student's *t*-test with extremely small sample sizes. PARE 18, 1–12.

Dijkstra, J.R., van Kempen, L.C., Nagtegaal, I.D., Bustin, S.A., 2013. Critical appraisal of quantitative PCR results in colorectal cancer research: can we rely on published qPCR results? Mol. Oncol. 8, 813–818.

Escuret, V., Collins, P.J., Casalegno, J.S., Vachieri, S.G., Cattle, N., Ferraris, O., Sabatier, M., Frobert, E., Caro, V., Skehel, J.J., Gamblin, S., Valla, F., Valette, M., Ottmann, M., McCauley, J.W., Daniels, R.S., Lina, B., 2014. A Novel I221L substitution in neuraminidase confers high-level resistance to Oseltamivir in influenza B viruses. J. Infect. Dis. 210, 1260–1269.

Ghedin, E., Holmes, E.C., DePasse, J.V., Pinilla, L.T., Fitch, A., Hamelin, M.E., Papenburg, J., Boivin, G., 2012. Presence of Oseltamivir-resistant pandemic A/H1N1 minor variants before drug therapy with subsequent selection and transmission. J. Infect. Dis. 206, 1504–1511.

Hayden, R.T., Hokanson, K.M., Pounds, S.B., Bankowski, M.J., Belzer, S.W., Carr, J., Diorio, D., Forman, M.S., Joshi, Y., Hillyard, D., Hodinka, R.L., Nikiforova, M.N., Romain, C.A., Stevenson, J., Valsamakis, A., Balfour Jr., H.H., 2008. Multicenter comparison of different real-time PCR assays for quantitative detection of Epstein-Barr virus. J. Clin. Microbiol. 46, 157–163.

Hayden, R.T., Gu, Z., Ingersoll, J., Abdul-Ali, D., Shi, L., Pounds, S., Caliendo, A.M., 2013. Comparison of droplet digital PCR to real-time PCR for quantitative detection of cytomegalovirus. J. Clin. Microbiol. 51, 540–546.

Hayden, R.T., Gu, Z., Sam, S.S., Sun, Y., Tang, L., Pounds, S., Caliendo, A.M., 2015. Comparative evaluation of three commercial quantitative cytomegalovirus standards by use of digital and real-time PCR. J. Clin. Microbiol. 53, 1500–1505.

Hindson, B.J., Ness, K.D., Masquelier, D.A., Belgrader, P., Heredia, N.J., Makarewicz, A.J., Bright, I.J., Lucero, M.Y., Hiddessen, A.L., Legler, T.C., Kitano, T.K., Hodel, M.R., Petersen, J.F., Wyatt, P.W., Steenblock, E.R., Shah, P.H., Bousse, L.J., Troup, C.B., Mellen, J.C., Wittmann, D.K., Erndt, N.G., Cauley, T.H., Koehler, R.T., So, A.P., Dube, S., Rose, K.A., Montesclaros, L., Wang, S., Stumbo, D.P., Hodges, S.P., Romine, S., Milanovich, F.P., White, H.E., Regan, J.F., Karlin-Neumann, G.A., Hindson, C.M., Saxonov, S., Colston, B.W., 2011. High-throughput droplet digital PCR system for absolute quantification of DNA copy number. Anal. Chem. 83, 8604–8610.

Hindson, C.M., Chevillet, J.R., Briggs, H.A., Gallichotte, E.N., Ruf, I.K., Hindson, B.J., Vessella, R.L., Tewari, M., 2013. Absolute quantification by droplet digital PCR versus analog real-time PCR. Nat. Methods 10, 1003–1005.

Leibovitch, E.C., Brunetto, G.S., Caruso, B., Fenton, K., Ohayon, J., Reich, D.S., Jacobson, S., 2014. Coinfection of human herpesviruses 6A (HHV-6A) and HHV-6B as demonstrated by novel digital droplet PCR assay. PLoS ONE 9, e92328.

McDermott GP1, Do, D., Litterst, C.M., Maar, D., Hindson, C.M., Steenblock, E.R., Legler, T.C., Jouvenot, Y., Marrs, S.H., Bemis, A., Shah, P., Wong, J., Wang, S., Sally, D., Javier, L., Dinio, T., Han, C., Brackbill, T.P., Hodges, S.P., Ling, Y., Klitgord, N., Carman, G.J., Berman, J.R., Koehler, R.T., Hiddessen, A.L., Walse, P., Bousse, L., Tzonev, S., Hefner, E., Hindson, B.J., Cauly 3rd, T.H., Hamby, K., Patel, V.P., Regan, J.F., Wyatt, P.W., Karlin-Neumann, G.A., Stumbo, D.P., Lowe, A.J., 2013. Multiplexed target detection using DNA-binding dye chemistry in droplet digital PCR. Anal. Chem. 85, 11619–11627.

Oxnard, G.R., Paweletz, C.P., Kuang, Y., Mach, S.L., O'Connell, A., Messineo, M.M., Luke, J.J., Butaney, M., Kirschmeier, P., Jackman, D.M., Jänne, P.A., 2014. Noninvasive detection of response and resistance in EGFR-mutant lung cancer using quantitative next-generation genotyping of cell-free plasma DNA. Clin. Cancer Res. 20, 1698–1705.

Persson, K., Hamby, K., Ugozzoli, L.A., 2005. Four-color multiplex reverse transcription polymerase chain reaction—overcoming its limitations. Anal. Biochem. 344, 33–42.

Pinilla, L.T., Holder, B.P., Abed, Y., Boivin, G., Beauchemin, C.A., 2012. The H275Y neuraminidase mutation of the pandemic A/H1N1 influenza virus lengthens the eclipse phase and reduces viral output of infected cells, potentially compromising fitness in ferrets. J. Virol. 86, 10651–10660.

Pizzorno, A., Bouhy, X., Abed, Y., Boivin, G., 2011. Generation and characterization of recombinant pandemic influenza A(H1N1) viruses resistant to neuraminidase inhibitors. J. Infect. Dis. 203, 25–31.

Rački, N., Dreo, T., Gutierrez-Aguirre, I., Blejec, A., Ravnikar, M., 2014. Reverse transcriptase droplet digital PCR shows high resilience to PCR inhibitors from plant, soil and water samples. Plant Methods 10, 1–10.

Sanmamed, M.F., Fernández-Landázuri, S., Rodríguez, C., Zárate, R., Lozano, M.D., Zubiri, L., Perez-Gracia, J.L., Martín-Algarra, S., González, A., 2015. Quantitative cell-free circulating BRAFV600E mutation analysis by use of droplet digital PCR in the follow-up of patients with melanoma being treated with BRAF inhibitors. Clin. Chem. 61, 297–304.

Svec, D., Tichopad, A., Novosadova, V., Pfaffl, M.W., Kubista, M., 2015. How good is a PCR efficiency estimate: recommendations for precise and robust qPCR efficiency assessments. Biomol. Detect. Quantif. 3, 9–16.

Taylor, S.C., Berkelman, T., Yadav, G., Hammond, M., 2013. A defined methodology for reliable quantification of Western blot data. Mol. Biotechnol. 55, 217–226.

Taylor, S.C., Mrkusich, E.M., 2014. The state of RT-quantitative PCR: firsthand observations of implementation of minimum information for the publication of quantitative real-time PCR experiments (MIQE). J. Mol. Microbiol. Biotechnol. 24, 46–52.

Thomas, R.K., Nickerson, E., Simons, J.F., Jänne, P.A., Tengs, T., Yuza, Y., Garraway, L.A., LaFramboise, T., Lee, J.C., Shah, K., O'Neill, K., Sasaki, H., Lindeman, N., Wong, K.K., Borras, A.M., Gutmann, E.J., Dragnev, K.H., DeBiasi, R., Chen, T.H., Glatt, K.A., Greulich, H., Desany, B., Lubeski, C.K., Brockman, W., Alvarez, P., Hutchison, S.K., Leamon, J.H., Ronan, M.T., Turenchalk, G.S., Egholm, M., Sellers,

W.R., Rothberg, J.M., Meyerson, M., 2006. Sensitive mutation detection in heterogeneous cancer specimens by massively parallel picoliter reactor sequencing. Nat. Med. 7, 852–855.
Watzinger, F., Suda, M., Preuner, S., Baumgartinger, R., Ebner, K., Baskova, L., Niesters, H.G., Lawitschka, A., Lion, T., 2004. Real-time quantitative PCR assays for detection and monitoring of pathogenic human viruses in immunosuppressed pediatric patients. J. Clin. Microbiol. 42, 5189–5198.
Zhang, T., Grenier, S., Nwachukwu, B., Wei, C., Lipton, J.H., Kamel-Reid, S., 2007. Inter-laboratory comparison of chronic myeloid leukemia minimal residual disease monitoring: summary and recommendations. J. Mol. Diagn. 4, 421–430.
Zhao, H., Wilkins, K., Damon, I.K., Li, Y., 2013. Specific qPCR assays for the detection of orf virus, pseudocowpox virus and bovine papular stomatitis virus. J. Virol. Methods 194, 229–234.